Two-Stage Performance of Polarization-Maintaining Holmium-Doped Fiber Amplifiers

Robert E. Tench [ID], *Senior Member, IEEE*, Clement Romano [ID], Glen M. Williams, Jean-Marc Delavaux, Thierry Robin [ID], Benoit Cadier, and Arnaud Laurent

Abstract—We report the experimental demonstration and record performance of two-stage broadband, high gain polarization-maintaining (PM) Ho-doped fiber amplifiers (HDFAs) at a signal wavelength of $\lambda_s = 2051$ nm. We begin by presenting a new PM Ho-doped fiber with core diameter 8 μm, a PANDA structure, a cutoff wavelength of 1650 nm, and a peak absorption of 57 dB/m at 1951 nm. Next, we consider architectures for high gain PM HDFAs. Here we demonstrate $G = 60$ dB with a dynamic range of >40 dB and noise figures as low as 10 dB. We then investigate configurations for high output power PM HDFAs. With one stage, we measure $P_{out} = 3.45$ W and an optical–optical slope efficiency $\eta = 69\%$. With two stages, we obtain $P_{out} = 6.7$ W and $\eta = 80\%$. The potential bandwidth of the high power PM HDFA is BW = 100 nm (7.5 THz). An optical signal-to-noise ratio of 58 dB/0.1 nm is achieved, and the polarization extinction ratio is >20 dB. Initial comparisons of simulations of gain and output power with our experimental results show relatively good agreement.

Index Terms—Doped fiber amplifiers, holmium, infrared fiber optics, optical fiber devices, polarization maintaining fiber, 2 microns.

I. INTRODUCTION

ATMOSPHERIC sensing [1], LIDAR [2], [3], and also high capacity WDM transmission system experiments [4]–[7] in the 2000 nm band all illustrate the need for wide bandwidth, high gain optical amplifiers in this region. Holmium-doped fiber amplifiers (HDFAs) are quite attractive in this area because they extend the bandwidth response toward long wavelengths of 2000–2150 nm. In addition, HDFAs exhibit high gain for wavelengths greater than 2050 nm, a region where Tm-doped fiber amplifiers have been found to exhibit low gain.

Several recent papers have reported results for both amplifiers and lasers using single stage, single mode Ho-doped fibers.

Filatova et al. [8] demonstrated G > 35 dB and $P_{out} = 1$ W with an amplifier pumped at 1125 nm, while Simakov et al. [9], [10] have reported G = 40 dB, $P_{out} = 0.25$ W, and noise figures NF = 7–14 dB with HDFAs pumped at 1950–2008 nm. Hemming et al. [11] have demonstrated a Holmium-doped fiber laser operating at 2090 nm and pumped at 1950 nm with an optical-optical slope efficiency of 87%.

While these recent results are encouraging, we propose here to extend and enhance the performance of existing HDFAs by using a two-stage PM configuration. A combination of high gain and large dynamic range are highly desirable for amplifiers in LIDAR systems. For this reason, it is important to design HDFAs which exhibit these characteristics. A large dynamic range is important because the single frequency semiconductor laser sources available in the 2000–2150 nm region exhibit relatively low output powers of only a few mW CW. Also, the primary applications of CO_2 sensing at 2051 nm and LIDAR, as well as the secondary application of transmitter power booster amplifiers in WDM transmission systems, can require a linearly polarized output. Therefore, the design and development of PM Ho-doped fiber is an important topic for research and development.

In this paper, we propose and demonstrate a new PM Ho-doped fiber, and new two-stage PM HDFA architectures designed for low average power laser signals. The new PM fiber is designed for full compatibility with components and devices used in current optical amplifier architectures. Our subsequent experimental investigation demonstrates PM HDFAs in one- and two-stage configurations for a signal wavelength of $\lambda_s = 2051$ nm and pump wavelengths $\lambda_p \approx 1950$ nm. Our single clad, single mode PM HDFAs [12] achieve a unique combination of record performance with gain G = 60 dB, a bandwidth BW of 100 nm (7.5 THz), an optical signal to noise ratio of OSNR = 58 dB, an optical-optical slope efficiency of $\eta = 80\%$, an output power $P_{out} = 6.7$ W, and dynamic range > 40 dB.

The organization of our paper is as follows: first, we report on a new PM Ho-doped fiber designed for high gain amplification in the 2000–2150 nm wavelength band. Next, we consider a two-stage amplifier architecture to optimize gain and dynamic range. Finally, we evaluate a two-stage amplifier optimized for optical power conversion efficiency and high output power. We also compare experiment and simulation, with a two-level model, using fiber spectral data derived from the manufacturer and from the literature.
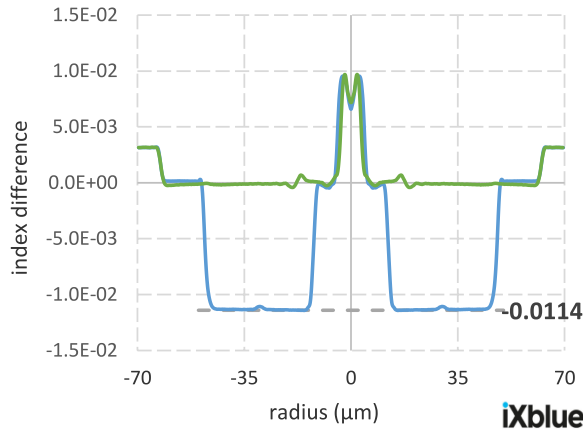
Fig. 1.   Refractive index profile of the slow and fast axis of the PM HDF.

Fig. 2.   Photograph of the end face of the PM HDF. The cladding diameter is 125 μm.

II. DATA FOR THE POLARIZATION-MAINTAINING HOLMIUM-DOPED FIBER

The fiber was manufactured at iXblue Photonics and its design targeted 5 main characteristics: high core absorption at pump wavelength, high power conversion efficiency (PCE), high core transparency at the signal wavelength, single mode operation above 1900 nm, and finally a large birefringence for robust polarization operation. The preform was manufactured using the well-known Modified Chemical Vapor Deposition (MCVD) technique [13] and more precisely the solution doping variant for rare-earth addition to the silica based core. We chose the alumino-silicate core composition which limits, for large rare-earth incorporation, detrimental effects on PCE such as ion-pairing and clustering [14].

The refractive index profile of the fiber is given in Figure 1. The numerical aperture calculated from the profile is found to be 0.15 which, with a fiber core diameter of 8 μm yields a cutoff wavelength of 1650 nm ensuring single mode operation with negligible bending losses at both pump and signal wavelength. The holmium core doping level was 0.5 Wt-% resulting in a core absorption of 57 dB/m at 1950 nm.

In terms of core transparency, we optimized the doping process to ensure minimum hydroxyl (OH) content. We measured, using the classic cutback method at 1380 nm, an OH content of 0.02 ppm ensuring negligible excess OH absorption at 2050 nm [15]. The background losses of the fiber were found to be 4 dB/km at 1310 nm but could not be precisely measured due to the high residual rare-earth absorption at the signal wavelength. We thus manufactured a passive fiber with identical core composition, with the notable exception of Holmium, and identical opto-geometric parameters and found the background attenuation at 2050 nm to be below 100 dB/km. Finally, we used a panda structure to obtain polarization maintaining operation for the final fiber, presented in Figure 2, which exhibits a birefringence of 3.3×10^{-4}.

Summary data for the new iXblue PM Ho-doped single clad silica fiber in our experiments are given below in Table I.

Fusion splice losses between this fiber and Coherent/Nufern PM1950 passive polarization-maintaining fiber were 0.1 dB or less.
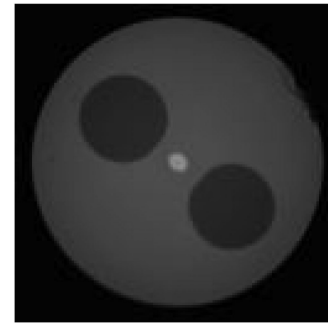
TABLE I
PM HO-DOPED FIBER DATA

Fiber ID	IXF-HDF-PM-8-125
Core Diameter, μm	8
Cladding Diameter, μm	125
Numerical Aperture	0.15
Fiber Structure	PANDA
Birefringence	3.3×10^{-4}
Background Loss, dB/m	0.2
Peak Absorption, dB/m	57 @ 1951 nm
Ion Pairing Coefficient, %	10 (Ref. [15])
$^5I_7$-$^5I_8$ Radiative Lifetime, mS	9.67 (Ref. [19])
$^5I_7$-$^5I_8$ Nonradiative Lifetime, mS	0.60

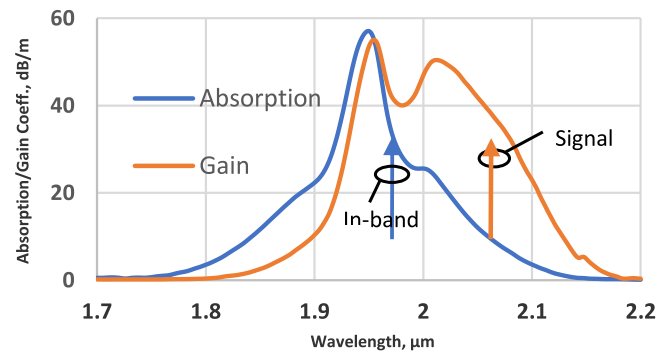

Fig. 3.   Gain and absorption spectra for the Ho-doped fiber.

Figure 3 shows gain and absorption spectra for the $^5I_7$-$^5I_8$ transition of the Ho-doped fiber, which were derived from measurements by iXblue and data from the literature [13]. The spectral region where the fiber exhibits significant gain clearly extends beyond 2150 nm.

Simulations of fiber performance used the gain and absorption spectra in Figure 3 and the data from Table I in a two-level Giles model [16] with a saturation parameter of 2.13×10^{18} m^{-1} s^{-1}. The ion pairing coefficient accounts for loss of excited state ions caused by detrimental pairwise interactions [17]. In our experiments we chose in-band pumping with $\lambda_p \approx 1950$ nm, close to the peak of the absorption as illustrated by the vertical blue arrow in Figure 1.
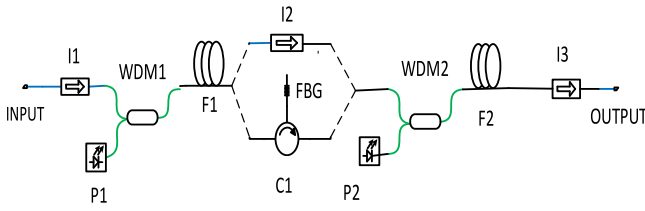
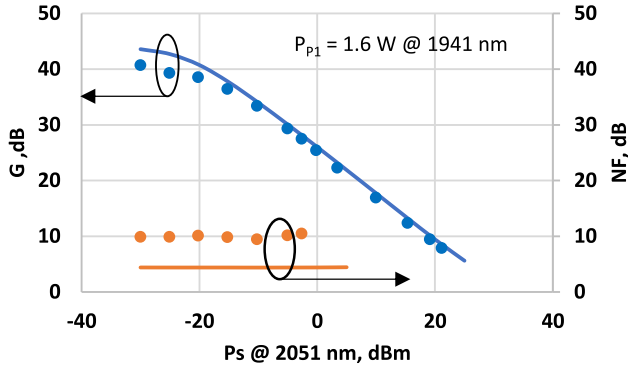Fig. 4.   Experimental setup for high gain and high output power PM HDFAs.

Fig. 5.   Gain and NF for the first stage of the high gain PM HDFA.

Fig. 6.   Gain and NF for the two-stage high gain PM HDFA.

III. EXPERIMENTAL SETUP FOR HIGH GAIN AND HIGH OUTPUT POWER PM HDFAS

The experimental configuration for the PM HDFAs studied is shown schematically in Figure 4.

Here, a multiwatt PM pump P1 at ≈ 1950 nm is combined in a multiplexer (WDM1) with a 2051.45 nm single frequency input signal P_s ($\Delta \nu < 1$ MHz, Eblana Photonics EP2051) which is then amplified by F1. Light from another multiwatt PM pump P2 at ≈ 1950 nm is combined in WDM2 with the output signal from F1 which is amplified by F2. The PM Ho-doped fibers, F1 and F2, have L1 = 1.8 m or 3.0 m, for high output power and high gain configurations, respectively; L2 is kept constant at 2.0 m.

In this setup, the first amplifying stage F1 functions as a preamplifier, while the second stage F2 is a power amplifier. Isolators I1 and I3 in the signal path ensure unidirectional operation and suppress backward ASE. Two interstage signal path elements are used: either a wideband isolator I2, or an ASE filter made of circulator C1 and a 1 nm wide reflection FBG centered at 2051.45 nm. Signal and pump powers and noise figures are measured internally, and linearly polarized signal and pump light propagate through the amplifier along the slow fiber axis.

IV. HIGH GAIN PM HDFA: EXPERIMENTAL RESULTS AND SIMULATIONS

Our first studies were for a high gain PM HDFA with L1 = 3.0 m and L2 = 2.0 m. Figure 5 plots the experimental gain and noise figure (points) as a function of input signal power P_s for the first stage of the high gain HDFA, for a pump power P1 = 1.6 W @ 1941 nm from a PM fiber laser source. Input powers greater than 0 dBm were achieved by amplifying the Eblana source with a Tm-doped fiber amplifier. A small signal gain G of 40 dB was observed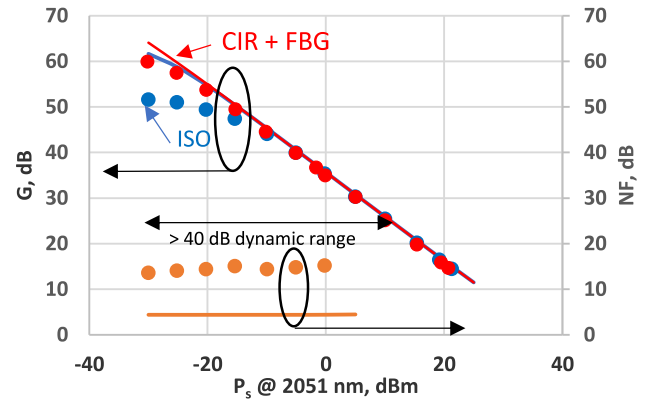, and the noise figure NF was constant with P_s at 10 dB across the dynamic range of the amplifier. Definitions of G and NF for the amplifier are given in detail in Eqns. 1–4 of [18].

For G > 25 dB, the dynamic range of the first stage amplifier is > 30 dB. Simulations of the first stage gain and noise figure, using the parameters from Table I and the spectra from Figure 3, are shown in solid lines. The gain agrees reasonably well with the data, while the measured noise figure is somewhat higher than the simulated value of 4.4 dB. This NF discrepancy is under active investigation. We note that the simulated noise figure value of 4.4 dB is higher than the theoretical limit of 3 dB for a high gain amplifier because of the proximity of the pump wavelength of 1941 nm to the signal wavelength of 2051 nm which creates a less than total inversion in the two level system.

Experimental data for the two-stage high gain HDFA are plotted in points in Figure 6. Here two interstage elements were used: isolator I1, with gain data shown in blue, or circulator C1/FBG, with gain data shown in red. For these data, P1 = 1.6 W @ 1952 nm from a PM MOPA source, and P2 = 5.0 W @ 1941 nm from a PM fiber laser source. A maximum gain of 60 dB was observed for the interstage BPF, and this was reduced to 52 dB with interstage isolator I2. For G > 25 dB, the two-stage amplifier had a dynamic range of > 40 dB. A noise figure of 14.5 dB was measured for the two-stage high gain HDFA (orange points). We attribute this high noise figure to excess low frequency ASE noise on the MOPA pump source used for P1, and this large value of noise figure is under investigation.

Simulations of gain and NF for the two-stage high gain HDFA are shown in solid lines in Figure 6. We observe that the gain simulations diverge somewhat from experimental measurements for low values (<−20 dBm) of P_s. The calculated NF of 4.4 dB is the same as for the first amplifier stage as expected from theory.

V. HIGH OUTPUT POWER PM HDFA: EXPERIMENTAL RESULTS AND SIMULATIONS

Our next investigations were for a high output power PM HDFA designed for $P_s > 0$ dBm. With these relatively high input power levels in mind, L1 was shortened to from 3.0 to 1.8 m, and L2 remained 2.0 m. The interstage optical element was isolator I2 only.

Figure 7 shows plots of output power P_{out} vs. pump power P_{P1}, for several levels of P_s, for the first stage F1. The
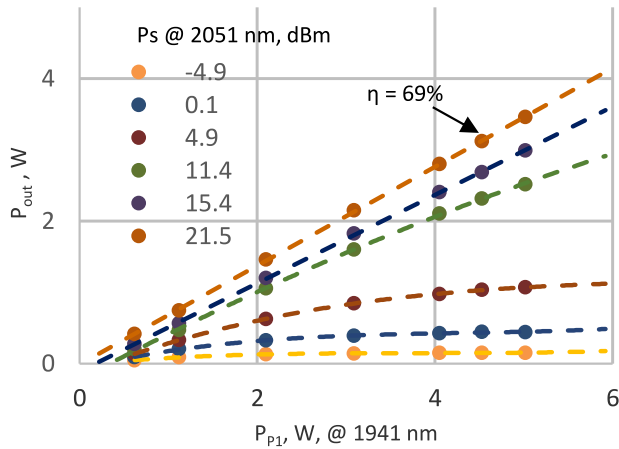
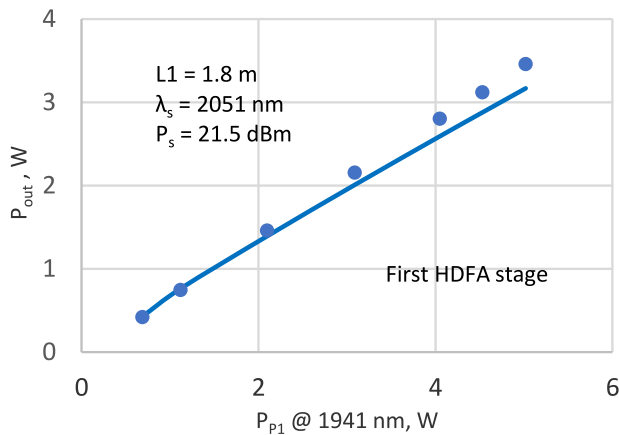Fig. 7. P_{out} vs. P_{P1}, as a function of P_s, for the first stage of the high output power PM HDFA.

Fig. 8. Comparison of experiment and simulation for the first stage of the high output power configuration.

Fig. 9. P_{out} vs. P_{P2}, as a function of P_s, for the two-stage high output power PM HDFA.

Fig. 10. Comparison of experiment and simulation for the two-stage high output power configuration.

experimental data in Figure 7 are represented by points, and the dashed lines are polynomial fits to the data. At the maximum input power of $P_s = 21.5$ dBm, a maximum P_{out} of 3.45 W was achieved for $P_{P1} = 5.0$ W @ 1941 nm. These data yield a high optical-optical slope efficiency of $\eta = 69\%$, where $\eta = \Delta P_{out}/\Delta P_p$ is the ratio of change in the output power P_{out} to change in the pump power P_p.

A comparison of simulation and experiment for the first stage of the high power amplifier is given in Figure 8. Here $P_s = 21.5$ dBm, the experimental data are given by points, and the solid curve is the simulation. Agreement between experiment and simulation is good, with a maximum deviation of 0.4 dB at the highest pump power of 5.0 W.

Figure 9 shows P_{out} vs. P_{P2}, as a function of P_s, for the two-stage high power HDFA configuration. For these measurements, $P_{P1} = 1.6$ W @ 1952 nm. The experimental data are represented by points, and the dashed lines indicate linear fits to the data. As shown by the values in Figure 9, a maximum output power of 6.7 W was achieved with a slope efficiency η of 80%. To our knowledge, this represents the highest slope efficiency so far reported for a PM Ho-doped fiber amplifier.

In Figure 10, we plot a comparison of experiment and simulation for the two-stage high power PM HDFA. For these data,
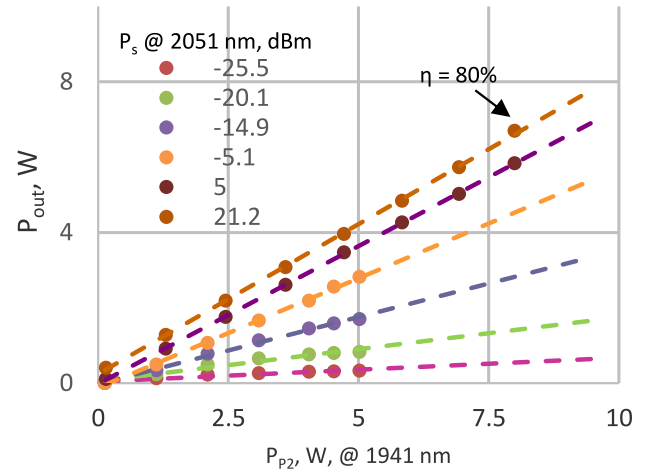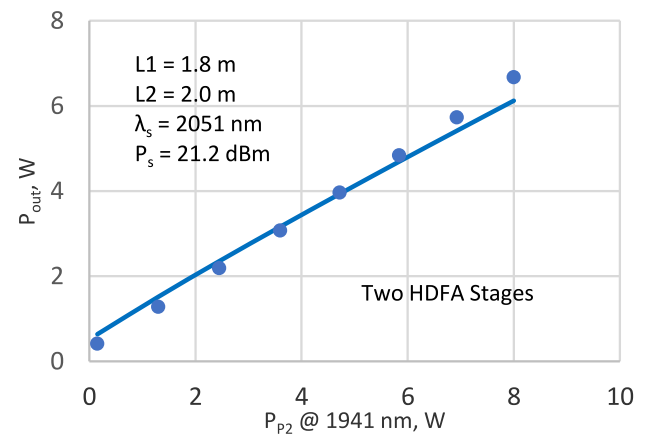
$P_s = 21.2$ dBm, and $P_{P1} = 1.6$ W @ 1952 nm. The experimental data are plotted with points and the simulation is given by the solid curve. Again, we note that the agreement between experiment and theory is good, with deviations of 0.4 dB at $P_{P2} = 8.0$ W and -0.1 dB at $P_{P2} = 0.4$ W.

From the output power data in Figures 7 and 9, we derive values of slope efficiency η for the one- and two-stage configurations, as shown in Figure 11. Here the experimental data are plotted in points, and the dashed lines are polynomial fits to the data. Using a threshold of 50% for slope efficiency as a criterion, we find that the required input powers are $P_s > +11$ dBm and $P_s > -10$ dBm for one and two stages, respectively. This behavior is caused by the significant gain compression that occurs in the two-stage configuration, and illustrates the considerable advantages of two-stage optical amplifier architectures. We note that the slope efficiency reaches an asymptotic maximum of 80%, indicating that the two-stage configuration is optimized for high power conversion efficiency.

Now we turn to measurements of the long-term stability of output power for the two stage HDFA configuration. Figure 12 shows a measurement of P_{out} vs. time for an elapsed time of six hours at $P_{out} = 6.7$ W. The measured variation in P_{out} over six
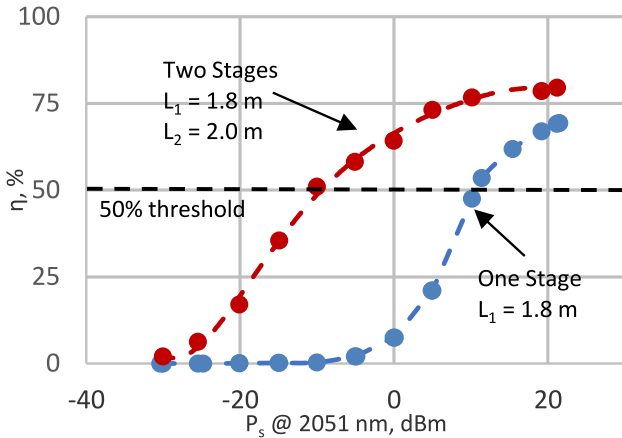
Fig. 11.   Slope efficiency η vs. Ps for one- and two-stage high output power PM HDFAs.
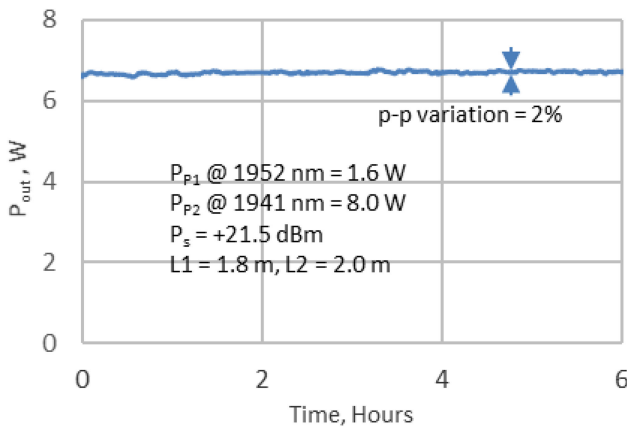

Fig. 12.   Long-term stability of P_{out} for the two-stage high output power HDFA.
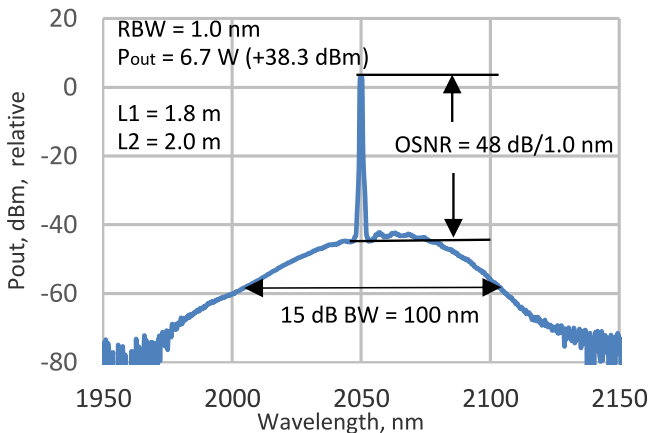

Fig. 13.   Output spectrum for the two-stage high output power PM HDFA.

hours is 2% p-p, a value which is consistent with measurements made on other 2000 nm band fiber amplifiers in our laboratory [20]. This measurement demonstrates the long-term stability of our amplifier design.

Finally, we look at the output spectrum of the two-stage high power HDFA. As illustrated in Figure 13, for $P_{out} = 6.7$ W, the measured optical signal-to-noise ratio (OSNR) is 58 dB/0.1

nm. This is a good operating value for power amplifiers in LIDAR and lightwave transmission systems. The estimated operating spectral bandwidth of the amplifier is found to be 100 nm (7.5 THz) by measuring the width of the background ASE spectrum under the peak of the optical signal [18]. The polarization extinction ratio (PER) of the two-stage PM high power amplifier is > 20 dB and is determined by the performance of output isolator I3.

In all of our measurements, no stimulated Brillouin scattering or other nonlinear effects were observed, up to the highest experimental value $P_{out} = 6.7$ W CW.

VI. DISCUSSION

In our experimental setup, the slow axis of the PM fiber was chosen to be consistent with the standard industry choice for axis of propagation. The linearly polarized pump laser at 1941 nm was aligned with the slow axis to investigate amplifier performance with co-linearly polarized pump and signal sources. Future experiments will study the effect of orthogonal pump and signal polarizations as well as the effect of an unpolarized pump source.

The high measured internal gains of 60/52 dB achieved with the two-stage architecture represent a significant advance in the state of the art, compared to previous results [8]–[10]. Such a high small signal gain is promising for LIDAR applications where the power of the single frequency source laser at 2051 nm may be limited to 1 mW or less. Amplification to output powers of 5 W or greater will increase the achievable signal-to-noise ratio achievable in LIDAR systems. We note, for example, that the maximum transmitted laser output power in [1] was 100 mW, and that 5 W output power would increase the system signal-to-noise ratio by a factor of 50 (see Eq. 10 in [1]).

Simulations of gain for the one-and two-stage high gain HDFAs show relatively good agreement with experiment. Simulations of noise figure do not agree as well with experimental data. The origin of these differences may be as follows:

1) Our data for absorption and gain coefficients are derived both from initial measurements by the manufacturer and from published data on representative Ho-doped fibers in the literature. Future simulations will be carried out using coefficients measured solely for the PM Ho-doped fiber under investigation.

2) The choice of pump wavelength λ_p versus signal wavelength λ_s needs to be more fully studied, to determine the effect of these two parameters on noise figure.

3) The amplitude noise characteristics of the pump sources require more thorough characterization. In particular, the low frequency ASE intensity noise of the 1952 nm MOPA pump source employed for P1 in the two-stage high gain HDFA will be investigated and its effect on the noise figure of the amplifier will be determined.

For the high output power two-stage configuration, the observed slope efficiency of 80% and output power $P_{out} = 6.7$ W represent significant improvements over previously reported experimental results [8]–[10]. Initial simulations of output power performance agree well with the experimental data.

We observe that the initial simulation results for gain and output power agree relatively well with the experimental data. Our simulation capability therefore enables the future theoretical design of high gain, large dynamic range, high output power two stage PM HDFAs.

The estimated operating bandwidth of 100 nm (7.5 THz), which is derived from a measurement of the width of the background ASE spectrum below the signal peak [18], is highly promising for multiwavelength WDM transmission applications of the two-stage high power amplifier. Previous work in this area has demonstrated operating optical bandwidths of around 40 nm (3 THz) [6]. Future experiments and simulations will directly determine the operating bandwidth of the one-and two-stage PM HDFAs, using multiple wavelength single frequency sources in the 2000–2150 nm region.

VII. SUMMARY

We have reported the design, experimental performance, and initial simulations of one- and two-stage polarization-maintaining high gain and high output power Holmium-doped fiber amplifiers.

We first introduced a new polarization maintaining Ho-doped aluminosilicate fiber with a peak absorption of 57 dB/m at 1951 nm, a PANDA fiber structure, a background loss of 0.2 dB/m at 2000 nm, and a birefringence of 3.3×10^{-4}.

Next, we presented the performance of one- and two-stage high gain PM HDFA configurations. With these amplifiers, we achieved a one stage gain of 40 dB, a noise figure of 10 dB, and a dynamic range of >30 dB. For the two-stage high gain amplifier, we achieved gains as large as 60 dB, a noise figure of 14.5 dB, and a dynamic range > 40 dB. The high NF for the two-stage amplifier is attributed to a noisy 1952 nm MOPA pump source, an issue which will be corrected in future experiments.

Finally, we described the optical efficiency of one-and two-stage high output power PM HDFA configurations. For one amplifier stage, we achieved an output power of 3.45 W and a slope efficiency $\eta = 69\%$. For two amplifier stages, we achieved $P_{out} = 6.7$ W and $\eta = 80\%$. The long-term power stability of the amplifier was measured to be 2% p-p over a time interval of six hours. From the output spectrum of the amplifier, we obtained an OSNR of 58 dB/0.1 nm and an estimated operating bandwidth of 100 nm (7.5 THz). The polarization extinction ratio of the two-stage high power PM HDFA was > 20 dB.

For both the high gain and high output power amplifier configurations, we presented initial simulations of HDFA performance using spectral data from iXblue and from the literature. The initial gain and output power simulations agree relatively well with the measured amplifier performance.

No stimulated Brillouin scattering, or other nonlinear effects, were observed up to the maximum $P_{out} = 6.7$ W.

Taken together, the measured and simulated characteristics of the one- and two-stage PM HDFAs represent a significant advance in Ho-doped fiber amplifier design, and point the way toward future improvements in atmospheric sensing, LIDAR, and high capacity DWDM lightwave system experiments in the 2000–2150 nm region of the spectrum.

REFERENCES

[1] G. D. Spiers *et al.*, "Atmospheric CO_2 measurements with a 2 μm airborne laser absorption spectrometer employing coherent detection," *Appl. Opt.*, vol. 50, pp. 2098–2111, 2011.

[2] F. Gibert, A. Dumas, J. Rothman, D. Edouart, C. Cenac, and J. Pellegrino, "Performances of a HgCdTe APD based direct detection lidar at 2 μM. Application to dial measurements," *EPG Web Conf.*, vol. 176, 2018, Art. no. 01001.

[3] S. Ishii *et al.*, "Research and development for future space-based Doppler Wind Lidar," in *Proc. 18th Coherent Laser Radar Conf.*, University of Colorado, Boulder, CO, USA, Jun. 27–Jul. 1, 2016, Paper M-10.

[4] M. U. Sadiq *et al.*, "40 Gb/s WDM transmission over 1.15-km HC-PBGF using an InP-based Mach-Zehnder modulator at 2 μm," *J. Lightw. Technol.*, vol. 34, no. 8, pp. 1706–1711, Apr. 2016.

[5] H. Zhang *et al.*, "Dense WDM transmission at 2 μm enabled by an arrayed waveguide grating," *Opt. Lett.*, vol. 40, pp. 3308–3311, 2015.

[6] H. Zhang *et al.*, "100 Gbit/s WDM transmission at 2 μm: Transmission studies in both low-loss hollow core photonic bandgap fiber and solid core fiber," *Opt. Express*, vol. 23, pp. 4946–4951, 2015.

[7] H. Zhang *et al.*, "81 Gb/s WDM transmission at 2 μm over 1.15 km of low-loss hollow core photonics bandgap fiber," in *Proc. Eur. Conf. Opt. Commun.*, Cannes, France, Sep. 21–25, 2014, Paper P.5.20.

[8] S. A. Filatova, V. A. Kaminyn, V. B. Svetkov, O. I. Medvedkov, and A. S. Kurkov, "Gain spectrum of the Ho-doped fiber amplifier," *Laser Phys. Lett.*, vol. 12, 2015, Art. no. 095105.

[9] N. Simakov *et al.*, "High gain holmium-doped fibre amplifiers," *Opt. Express*, vol. 24, pp. 13946–13956, 2016.

[10] N. Simakov *et al.*, "Holmium doped fiber amplifier for optical communications at 2.05–2.13 μm," in *Proc. Opt. Fiber Commun. Conf. Exhib.*, Los Angeles, CA, USA, Mar. 22–26, 2015, Paper Tu2C.6.

[11] A. Hemming, N. Simakov, M. Oermann, A. Carter, and J. Haub, "Record efficiency of a holmium-doped silica fibre laser," in *Proc. Conf. Lasers Electro-Opt.*, San Jose, CA, USA, Jun. 5–10, 2016, Paper SM3Q.5.

[12] R. E. Tench, C. Romano, J.-M. Delavaux, T. Robin, B. Cadier, and A. Laurent, "Broadband high gain polarization-maintaining holmium doped fiber amplifiers," in *Proc. Eur. Conf. Opt. Commun.*, Rome, Italy, Sep. 23–27, 2018, Paper Mo3E.3.

[13] S. R. Nagel, J. B. MacChesney, and K. L. Walker, "An overview of the modified chemical vapor deposition (MCVD) process and performance," *IEEE J. Quantum Electron.*, vol. 18, no. 4, pp. 459–476, Apr. 1982.

[14] S. B. Poole, D. N. Payne, and M. E. Fermann, "Fabrication of low-loss optical fibers containing rare earth ions," *Electron. Lett.*, vol. 21, pp. 737–738, 1985.

[15] N. Simakov, A. Hemming, W. A. Clarkson, J. Haub, and A. Carter, "A cladding-pumped, tunable holmium doped fiber laser," *Opt. Express*, vol. 21, pp. 28415–28422, 2013.

[16] C. R. Giles, C. A. Burrus, D. DiGiovanni, N. K. Dutta, and G. Raybon, "Characterization of erbium-doped fibers and application to modeling 980-nm and 1480-nm pumped amplifiers," *IEEE Photon. Technol. Lett.*, vol. 3, no. 4, pp. 363–365, Apr. 1991.

[17] A. S. Kurkov, E. M. Sholokhov, A. V. Marakulin, and L. A. Minashina, "Effect of active-ion concentration on holmium fibre laser efficiency," *Quantum Electron.*, vol. 40, pp. 386–388, 2010.

[18] R. E. Tench, C. Romano, and J.-M. Delavaux, "Optimized design and performance of a shared pump single clad 2 μm TDFA," *Opt. Fiber Technol.*, vol. 42, pp. 18–23, 2018.

[19] R. Chen *et al.*, "Thermal and luminescent properties of 2-μm emission in thulium-sensitized holmium-doped silicate germanate glass," *Photon. Res.*, vol. 4, pp. 214–221, 2016.

[20] R. E. Tench, C. Romano, and J.-M. Delavaux, "Broadband 2-W output power tandem thulium-doped single clad fiber amplifier at 2 μm," *IEEE Photon. Technol. Lett.*, vol. 30, no. 5, pp. 503–506, Mar. 2018.

Authors' biographies not available at the time of publication.